NMR investigation of the diffusion and conduction properties of the semiconductor tellurium. I. Electronic properties

H. Selbach and O. Kanert
Physikalisches Institut, Universität Dortmund, 46 Dortmund 50, West Germany

D. Wolf
Materials Science Division, Argonne National Laboratory, Argonne, Illinois 60439

(Received 14 November 1978)

The Knight shift and spin-lattice relaxation time of ^{125}Te in tellurium single crystals have been measured between room temperature and the melting point (724 K) using pulsed-NMR methods. Over the entire temperature range, the temperature dependence of the Knight shift is found to be determined completely by the intrinsic conductivity associated with thermally created conduction electrons in the conduction band, and the band-gap energy is determined. The spin-lattice relaxation time shows different temperature variations in two different regions: below 420 K ("low-temperature region"), spin-lattice relaxation is due to the conduction electrons (thus yielding information on the gap energy), while above 420 K ("high-temperature region") the relaxation process is due to the self-diffusion of Te atoms. Our Knight-shift results are found to agree quantitatively with a modified Knight-Korringa relation valid for semiconductors, which was originally derived by Bloembergen and which is reconsidered in the theoretical part of this article. The electronic contribution to spin-lattice relaxation is analyzed in terms of Hebel and Slichter's single spin-temperature theory as applied to semiconductors. The same gap energy, $E_g = 0.30$ eV, is found from both our Knight-shift and spin-lattice relaxation data. The self-diffusion properties of tellurium as extracted from our high-temperature relaxation studies will be the subject of a subsequent article.

I. INTRODUCTION

Tellurium is a semiconductor with very unusual properties.[1] In contrast to the "classical" semiconductors germanium and silicon, tellurium has a characteristically low crystal symmetry (see below), melting temperature ($T_m = 724$ K), Debye temperature ($\Theta_D = 129$ K), and small energy gap (see below).

Its NMR properties are also unique. The low natural abundance of the NMR isotopes ^{123}Te and ^{125}Te (0.85% and 6.98%, respectively) complicates the experimental investigation of NMR properties, but, on the other hand, simplifies the interpretation of experimental results in some cases, since direct and pseudodipolar nuclear-spin interactions play only a minor role in the very dilute spin system. Both isotopes have spin $I = \frac{1}{2}$. Therefore, quadrupolar interactions, which would otherwise be expected to be considerable in the noncubic crystal lattice, do not exist. The high number of core electrons is responsible for the very large chemical-shift interactions observed which, in more "normal" materials, are orders of magnitude smaller than the dipolar and quadrupolar interactions. For these reasons, tellurium offers a rather simple and convenient nuclear-spin system which may be used to investigate electronic and diffusional properties in the rather wide temperature range between room temperature and the melting point.

The hexagonal crystal structure of tellurium (trigonal system) consists of spiral chains. Every fourth atom sits directly above another atom in the same chain. The chains are centered around the ⟨0001⟩ direction (c axis). Neighboring atoms on the same chain are rotated by 120° with respect to one another. Therefore, each chain appears triangular when viewed along the c direction (see Fig. 1). The distance between the two nearest neighbors in any chain is 2.86 Å, and that between adjacent chains (four such neighbors per atom) is 3.46 Å. While the bonds between different chains are of the Van der Waals type (with binding energies between atoms on neighboring chains ranging between 0.22 and 0.05 eV),[1] the bonds between neighboring atoms on the same chain are covalent (with a binding energy of about 0.68 eV).[1]

The intrinsic electronic properties of tellurium may be characterized by the energy gap E_g between the

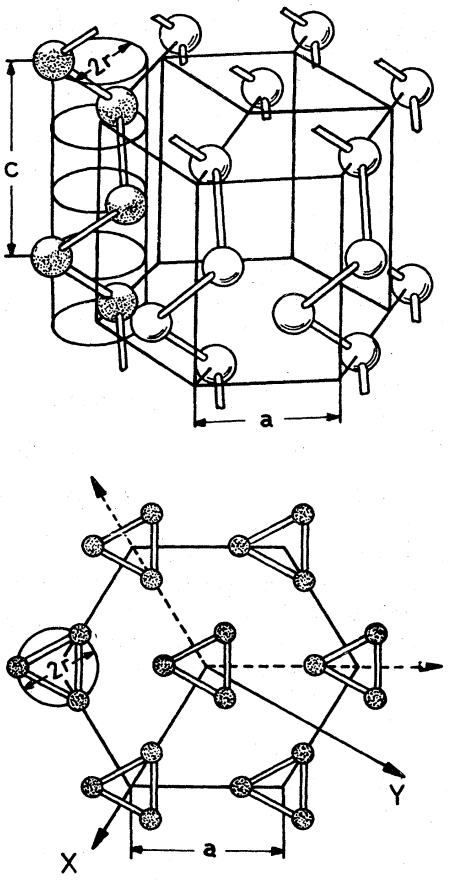

FIG. 1. Crystal structure of tellurium consisting of spiral chains arranged in a hexagonal lattice (top). The three nonequivalent atom sites lead to a three-line NMR spectrum of ^{125}Te due to chemical-shift interaction. The lattice parameters are $a = 4.45$ Å, $c = 5.95$ Å, and $r = 1.19$ Å. In the bottom half, a view along the c axis illustrates the hexagonal arrangement of the triangular spiral chains.

valence band and the conduction band.[1] Optical absorption measurements[2] show a decrease of E_g from about 0.34 eV at 100 K to about 0.32 eV at 450 K. Optical-emission studies yield slightly smaller values of E_g (Ref. 2).

The relatively low lattice energy suggests that the thermal creation of point defects may play an important part in both the electronic conductivity and the self-diffusion properties. Thus, for example, if a bond within a chain is broken by the formation of a vacancy, an electronic acceptor state may be created, since the free Te bonds at the chain ends tend to be saturated by free electrons. By measuring the Hall coefficient after quenching and annealing of Te single crystals, Hörstel and Kretzschmar[3] investigated the temperature dependence of the acceptor concentration. They concluded that thermally created vacancies with an enthalpy of formation of about 0.8 eV are, indeed, the origin of the acceptor states.

The NMR spectrum of single-crystalline tellurium was first observed by Bensoussan[4] and Koma.[5] They found three well-separated absorption lines, each of which showed a highly anisotropic chemical shift. More recently, Selbach and Kanert[6] showed that even up to the melting point, these characteristics of the NMR spectrum do not change. The observed chemical-shift tensors have been related to the types of Te positions within each trigonal chain on which the orientations of the electronic bonds differ.[4,5] It was found that in their respective principal-axes systems, the three chemical-shift tensors on the three positions are identical.[4,5]

The three different chemical shifts observed, therefore, are the result of the different orientations of the tensor ellipsoids on the three types of Te positions within a chain. By varying the crystallographic orientation of the Zeeman field $\vec{H}_0$, it is therefore possible to vary the relative positions of the three NMR lines. Through an appropriate choice of orientations, two or even all three lines may be forced to coincide.[6] The observed chemical-shift tensors have been interpreted theoretically[7] in terms of the sp^3 hybridization of the valence-electron wave functions. Initial nuclear-spin-relaxation measurements of the low-temperature T_1 properties of tellurium (4 – 300 K) were reported by Koma *et al.*[8] Neither electronic nor diffusional effects on T_1 are found at these low temperatures, and T_1 appears to be determined by the phonon-induced time variation of the three chemical-shift tensors.

More recently, Selbach and Kanert[6] extended the temperature range considerably by measuring T_1 up to the melting temperature. Their measurements clearly demonstrate that in addition to the low-temperature region, two temperature regimes, in which T_1 is determined by different microscopic processes, may be distinguished: (a) At medium temperatures (300 – 420 K), T_1 is determined by thermally mobilized conduction electrons, (b) Above 420 K ("high-temperature region"), T_1 is dominated by diffusion-induced chemical-shift fluctuations.

In the present article and its sequel, a comprehensive experimental and theoretical investigation of the NMR behavior in these temperature regions is presented for high-purity tellurium single crystals. While the high-temperature (diffusion-induced) properties will be the subject of the second article, in the present paper the following three questions will be investigated: (a) Does tellurium exhibit a Knight shift of the NMR spectrum? If a Knight shift is found, how is its magnitude related to what is presently known about the electronic properties of tellurium?[1] (b) Can we detect an electronic contribution to T_1 which arises from the intrinsic conductivity of tellurium? (c) How large is the band gap (for intrinsic

conductivity) between the valence and the conduction band?

To answer these questions we have performed the first measurements, to our knowledge, of the spin-lattice relaxation and Knight-shift effects associated with the *intrinsic* conductivity of a semiconductor. The *extrinsic* conductivity of semiconductors has been the subject of earlier investigations (which do not, however, permit measurement of the gap energy).[9] As a starting point for the interpretation of our Knight-shift and T_1 measurements, the early theory of Bloembergen[10] will be reconsidered from a more general theoretical point of view.

II. THEORY OF NUCLEAR SPIN-LATTICE RELAXATION CAUSED BY CONDUCTION ELECTRONS IN SEMICONDUCTORS

A. Application of Hebel-Slichter theory

Among the first-order magnetic hyperfine interactions, the Fermi-contact interaction usually dominates the nuclear spin-lattice relaxation caused by conduction electrons in metals and semiconductors. For a crystal containing N_e conduction electrons and N identical nuclei, the Fermi-contact interaction Hamiltonian may be written as follows:

$$\mathcal{H}_{\rm FC}=\frac{8\pi\hbar^2}{3}\gamma_e\gamma_I\sum_{j=1}^{N}\sum_{m=1}^{N_e}\vec{I}_j\cdot\vec{S}_m\delta(\vec{r}_{jm})\ , \tag{2.1}$$

where γ_e and γ_I denote, respectively, the electronic and nuclear gyromagnetic ratios while $\hbar\vec{I}_j$ and $\hbar\vec{S}_m$ represent the angular-momentum operators of nucleus j and electron m, respectively. $\vec{r}_{jm}=\vec{r}_j-\vec{r}_m$ is the vector joining some electron m with some nucleus j. For the purpose of investigating spin-lattice relaxation processes, the Hamiltonian of the entire crystal may be subdivided into the Hamiltonians of the isolated nuclear-spin system $\mathcal{H}_S$, of the "lattice" $\mathcal{H}_L$ (including all nonnuclear-spin degrees of freedom), and the interaction Hamiltonian $\mathcal{H}_{SL}$ between these two reservoirs, according to

$$\mathcal{H}=\mathcal{H}_S+\mathcal{H}_L+\mathcal{H}_{SL}\ . \tag{2.2}$$

An isolated nuclear spin-$\frac{1}{2}$ system experiences mainly Zeeman, and rigid-lattice (RL) dipolar (and, for atoms with large electron cores, pseudodipolar) interactions; hence

$$\mathcal{H}_S=\mathcal{H}_Z+\mathcal{H}_D^{\rm RL}\ . \tag{2.3}$$

The spin-lattice relaxation rate $(T_1^{-1})_e$ arising from conduction electrons in a Zeeman field H_0 of arbitrary strength with respect to the dipolar local field H_D, is most conveniently deduced from the Hebel-Slichter equation.[11] Hence, by assigning a single spin temperature to the nuclear-spin reservoir and considering $\mathcal{H}_{SL}=\mathcal{H}_{\rm FC}$ as a weak perturbation which acts on $\mathcal{H}_S$, and performing a calculation outlined in detail in Ref. 12, we obtain

$$\left(\frac{1}{T_1}\right)_e=\frac{32}{9}\pi^2\gamma_e^2\gamma_I^2\hbar^4\frac{H_0^2+\delta H_D^2}{H_0^2+H_D^2}J_e^{(1)}(\Omega)\ , \tag{2.4}$$

where Ω represents the nuclear precession frequency associated with the combined effect of Zeeman and local-field precession. The spectral densities associated with the fluctuations of $\mathcal{H}_{\rm FC}$ which are experienced by the nuclear spins,

$$J_e^{(1)}(\omega)=\frac{1}{N{\rm Tr}_e(1)}\sum_{j=1}^{N}\sum_{m=1}^{N_e}\sum_{n=1}^{N_e}\int_{-\infty}^{+\infty}dt\,{\rm Tr}_e[S_m^{(+)}(t)S_n^{(-)}]\times\delta(\vec{r}_m(t)-\vec{r}_j(t))\times\delta(\vec{r}_n(0)-\vec{r}_j(0))\,e^{i\omega t}\ , \tag{2.5}$$

may be shown[13] to be independent of the nuclear precession frequency (which is much smaller than the precession frequency of the conduction electrons). Therefore, the field dependence of $(T_1^{-1})_e$ in Eq. (2.4) is entirely determined by the magnitude of the factor δ defined by

$$\delta=1+\frac{2H_D^{(0)}H_D^{(n)}}{H_D^2}\ , \tag{2.6}$$

where $H_D^{(0)}$ and $H_D^{(n)}$ denote, respectively, the secular and nonsecular contributions to H_D. As discussed in more detail in Ref. 12, in powders with only direct dipolar interactions between nuclear spins, we have

$$\langle(H_D^{(n)})^2\rangle=4\,\langle(H_D^{(0)})^2\rangle=\tfrac{4}{5}\langle H_D^2\rangle\ . \tag{2.7}$$

Here the parentheses symbolize a solid-angle average. Combining Eqs. (2.7) and (2.6), we thus find that in powders we have $\delta=1.8$, while in a single-crystal δ is expected to be anisotropic. In the high-field limit the fraction in Eq. (2.4) involving magnetic fields becomes unity, and the relaxation rate of the Zeeman reservoir becomes

$$\left(\frac{1}{T_1^Z}\right)_e=\frac{32}{9}\pi^2\gamma_e^2\gamma_I^2\hbar^4J_e^{(1)}(\Omega)\ . \tag{2.8}$$

Equation (2.8) agrees completely with Winter's result.[14] Combining Eqs. (2.8) and (2.4) we may write

$$\left(\frac{1}{T_1}\right)_e=\left(\frac{1}{T_1^Z}\right)_e\frac{H_0^2+\delta H_D^2}{H_0^2+H_D^2}\ . \tag{2.9}$$

In most cases in which δ has been determined experimentally, values between 2 and 3 have been found (see, for example, Refs. 15–17). As discussed in Ref. 12, values of δ in excess of 1.8 are expected for nuclei with quadrupolar moments only. Interestingly,

all metals in which δ has been determined so far have quadrupolar moments.

The spectral densities (2.5) have been calculated by Hebel and Slichter[11] (see also Ref. 13). When all but the Zeeman and kinetic energies of the electrons are neglected and the complete wave functions are decomposed into products of Bloch functions and nuclear-spin wave functions, a lengthy calculation[13] leads to

$$J_e^{(1)} = \frac{2\pi}{\hbar} \int_0^\infty \langle |u_{\vec{k}}(0)|^2 \rangle_E^2 \rho^2(E) \times f(E)[1-f(E)]\, dE \,, \tag{2.10}$$

where $\langle |u_{\vec{k}}(0)|^2 \rangle_E$ denotes the density of electrons with average energy E and wave-vector $\vec{k}$ at the nuclear positions averaged over the energy surface. $\rho(E)$ represents the electronic density of states, while $f(E)$ symbolizes the probability that a state of energy E is occupied by an electron.

Before Eq. (2.10) is evaluated for the intrinsic and extrinsic conductivity of semiconductors, its application to conduction electrons in metals will be reviewed briefly.

B. Correlation functions for metals

Since electrons in metals follow the laws of Fermi-Dirac statistics, $f(E)$ in Eq. (2.10) is to be identified with the corresponding distribution function. As shown by Hebel and Slichter, Eq. (2.10) then yields

$$J_e^{(1)} = \frac{2\pi}{\hbar} \langle |u_{\vec{k}}(0)|^2 \rangle_{E_F}^2 \rho^2(E_F)\, kT \,, \tag{2.11}$$

where E_F denotes the Fermi energy. By inserting the density of states for the quasi-free electron gas[18] and combining Eqs. (2.11) and (2.9), the following well-known relationship is obtained:

$$\begin{aligned} \frac{1}{T_1^Z} &= \tfrac{64}{9}\pi^3\hbar^3\gamma_e^2\gamma_I^2 \langle |u_{\vec{k}}(0)|^2 \rangle_{E_F}^2 \rho^2(E_F)\, kT \\ &= \tfrac{16}{3}\frac{\pi}{\hbar}\gamma_e^2\gamma_I^2 \langle |u_{\vec{k}}(0)|^2 \rangle_{E_F}^2 (m_e^*)^2 n_e^{2/3}\, kT \\ &= C_K T \,, \end{aligned} \tag{2.12}$$

where m_e^* is the effective mass of electrons and n_e their density, and C_K represents a constant first derived by Korringa.

C. Correlation functions for semiconductors

As is well known, inside the conduction band of a semiconductor ($E-E_F >> kT$) the Fermi-Dirac distribution function may be replaced by a Boltzmann distribution function. Electrons in the conduction band and holes in the valence band [the latter with distribution function $1-f(E)$] may therefore be treated according to classical statistics.

In the limit in which $E-E_F >> kT$, $f(E)$ is rather small and $1-f(E)$ practically equals unity. To a good approximation, the average electron density $\langle |u_{\vec{k}}(0)|^2 \rangle_E$ is a slowly varying function of E. Its value inside the conduction band is therefore approximately equal to its value near the bottom E_0 of the conduction band (for electrons) or near the top of the valence band (for holes). Equation (2.10) then simplifies as follows:

$$J_e^{(1)} = \frac{2\pi}{\hbar} \langle |u_{\vec{k}}(0)|^2 \rangle_{E_0}^2 \int_{E_g}^\infty \rho^2(E) f(E)\, dE \,. \tag{2.13}$$

Here E_g denotes the gap energy of the semiconductor. (Note that in the usual way the top of the valence band has been chosen to represent $E=0$.) Substitution of the density of states for a parabolic band into Eq. (2.13) yields

$$\left(\frac{1}{T_1^Z}\right)_e = \frac{128}{9}\frac{\gamma_e^2\gamma_I^2}{\pi\hbar^3} \langle |u_{\vec{k}}(0)|^2 \rangle_{E_0}^2 (m_e^*)^3 \times (kT)^2 e^{-(E_g-E_F)/kT} \,. \tag{2.14}$$

The s part of the electron-nucleus interaction not only gives rise to spin-lattice relaxation but also to a Knight-shift $K = \Delta H/H_0$ of the NMR line. As shown by Bloembergen,[10] this shift is proportional to the number n_e of electrons in the valence band (per unit volume), and[10]

$$K = \frac{\Delta H}{H_0} = \frac{8\pi}{3}\gamma_e^2\hbar^2 \langle |u_{\vec{k}}(0)|^2 \rangle_{E_0} \frac{n_e}{kT} \,. \tag{2.15}$$

For pure or doped semiconductors, n_e may be calculated as follows:[18]

$$\begin{aligned} n_e &= \int_{E_g}^\infty \rho(E)\, f(E)\, dE \\ &= \frac{2}{\hbar^3}(2\pi m_e^* kT)\, e^{-(E_g-E_F)/kT} \,. \end{aligned} \tag{2.16}$$

This expression may be introduced into Eq. (2.14) in order to eliminate E_F; we thus obtain

$$\left(\frac{1}{T_1^Z}\right)_e = C_B n_e T^{1/2} \,, \tag{2.17}$$

with the practically temperature-independent "Bloembergen constant" given by

$$C_B = \tfrac{512}{9}\pi^2\gamma_e^2\gamma_I^2 k^{1/2} \left(\frac{m_e^*}{2\pi}\right)^{3/2} \langle |u_{\vec{k}}(0)|^2 \rangle_{E_0}^2 \,. \tag{2.18}$$

Equations (2.17) and (2.18) were first derived by

Bloembergen[10] in a rather intuitive manner. For comparison with Bloembergen's results, it is useful to remember that in Bloembergen's expression for $\mathcal{H}_{FC}$, the hyperfine constant A (in units of the atomic volume V_A) is given by

$$AV_A = \frac{8\pi}{3}\hbar^2\gamma_e\gamma_I\langle|u_{\vec{k}}(0)|^2\rangle_{E_0} . \quad (2.19)$$

Comparing these results with those derived for a Fermi-Dirac gas, we observe that for conduction electrons, $(T_1^Z)_e^{-1}$ is proportional to $(m_e^*)^2 n_e^{2/3} T$ [see Eq. (2.12)], while for a semiconductor $(T_1^Z)_e^{-1}$ is proportional to $(m_e^*)^{3/2} n_e T^{1/2}$ [see Eqs. (2.17) and (2.18)]. A simple qualitative physical picture accounting for these features was discussed by Bloembergen.[10]

The above results are valid for any (doped or pure) semiconductor. In doped semiconductors, n_e is usually temperature independent and constant. Equation (2.17) may then be used directly to predict the explicit temperature variation of the spin-lattice relaxation rate. In pure semiconductors, however, the concentration of electrons and holes, n_e and n_h, increases strongly with increasing temperature, according to[18]

$$n_e = n_h = \frac{2}{h^3}(2\pi kT)^{3/2}(m_e^* m_h^*)^{3/4} e^{-E_g/2kT} , \quad (2.20)$$

and the Fermi energy lies approximately in the center of the band gap (i.e., $E_F \simeq \frac{1}{2}E_g$). Equations (2.17) and (2.15) then become, respectively,

$$\left(\frac{1}{T_1^Z}\right)_e = \frac{128}{9}\frac{\gamma_e^2\gamma_I^2}{\pi\hbar^3}\langle|u_{\vec{k}}(0)|^2\rangle_{E_0}^2 (m_e^*)^3 \times\left(\frac{m_h^*}{m_e^*}\right)^{3/4}(kT)^2\exp(-E_g/2kT) , \quad (2.21a)$$

$$K = \frac{\Delta H}{H_0} = \frac{2}{3\hbar\pi^2}(2\pi)^{3/2}\gamma_e^2\langle|u_{\vec{k}}(0)|^2\rangle_{E_0} \times(m_e^* m_h^*)^{3/4}(kT)^{1/2}\exp(-E_g/2kT) . \quad (2.21b)$$

Therefore, by measuring the temperature variation of the spin-lattice relaxation rate or the Knight-shift, the gap energy E_g may be determined.

To eliminate the electron density at the nuclear positions, by analogy with the Korringa relation for metals[13] expressions (2.21a) and (2.21b) may be combined to yield

$$K^2(T_1^Z)_e T = \frac{\hbar}{4k}\left(\frac{\gamma_e}{\gamma_I}\right)^2\left(\frac{m_\hbar^*}{m_e^*}\right)^{3/4} e^{-E_g/2kT} . \quad (2.22)$$

It should be noted at this point that γ_e, the gyromagnetic ratio of the conduction electrons, differs in general from that of free electrons. In particular, for tellurium the average g factor of the conduction electrons has a value of 9 instead of the free-electron value of 2 (Ref. 1).

III. EXPERIMENTAL DETAILS

The NMR measurements on ^{125}Te were performed at magnetic fields of 14 and 63 kG, respectively, using a Bruker pulse spectrometer SXP 4-100 including a transient recorder (Data Lab DL 905). The NMR system was connected to a Varian 620 1 on-line computer in order to generate the pulse sequence, and store and analyze the data. The relaxation time T_1^Z was measured by applying a π-pulse or a saturation-pulse sequence at a time τ prior to the $\frac{1}{2}\pi$ "reading" pulse, whereas the relaxation measurements at zero field were carried out by means of the ADRF (adiabatic demagnetization in the rotating frame) technique. The spectrum, as well as the Knight shift, of ^{125}Te were obtained from Fourier transformation of the off-resonance free-induction decay following a $\frac{1}{2}\pi$ pulse. The shift measurements have been referred to the ^{125}Te signal of solid $TeCl_2$.

Cylindrical samples, 4 mm in diameter and 10 mm in length, were prepared from tellurium single crystals, with the cylinder axis along the crystalline c direction. Two types of single crystals were used, namely Czochralski-grown crystals with a natural isotopic abundance of ^{125}Te (obtained from Wacker Chemitronic/Frankfurt, Germany and self-grown single crystals prepared from enriched (94% ^{125}Te) ultrapure tellurium by the zone-melting method described by Tao-I Chiang.[19]

The sample was mounted on a goniometer inside a high-temperature probe which was capable of operating at temperatures up to 700 ° C and could be temperature controlled with an accuracy of about ±1 ° C. The single platinum NMR coil was fitted into a quartz tube that was noninductively wound with a heater coil. The heater coil was driven by a power supply that was continuously controlled by a thermocouple-actuated temperature controller.

The entire probe assembly was mounted in a water-cooled copper container. The temperature of the sample was determined by means of a Philips Chromel-Alumel thermocouple placed in contact with the sample.

IV. EXPERIMENTAL RESULTS AND DISCUSSION

A. Shift measurements

As mentioned in Sec. III, the temperature dependence of the position of the measured ^{125}Te spectrum was referred to ^{125}Te in solid $TeCl_2$. The evaluation

of the experimental data shows that within the experimental error limit of ±10%, the chemical-shift tensor is independent of temperature over the entire temperature range (300–740 K). Due to the increasing number of conduction electrons, the center of mass of the rotation pattern of the three-line spectrum scales with temperature as described by Eq. (2.21b). Since the chemical-shift tensor is determined by the orbital electrons and hence by the crystal structure, it can be concluded that the crystal structure of tellurium remains practically unchanged up to the melting point. This is in agreement with the data of Arnold and Grosse,[20] who measured the relative temperature dependence of the lattice constants by x-ray methods.

Figure 2 shows the measured Knight shift of ^{125}Te in tellurium as a function of temperature in a representation suggested by Eq. (2.21b), with

$$K/T^{1/2} = A_1 \exp(-E_g/2kT) , \tag{4.1}$$

where A_1 is a temperature-independent constant. An expression for A_1 may be derived by comparing Eqs. (4.1) and (2.21b). The straight line in Fig. 2 indicates a uniform shift mechanism over the entire temperature range (room temperature to melting point) caused by the conduction electrons. The data points were found to be independent of the crystal orientation relative to the external field and of the concentration of the ^{125}Te isotope. The slope of the straight line in Fig. 2 leads to a gap energy E_g of 0.30 eV, in agreement with the gap energy of tellurium at higher temperatures.[1] The experimental value of the coefficient A_1 in Eq. (4.1) is determined from Fig. 2 to be

$$A_1 = 1.38 \times 10^{-4} \mathrm{K}^{-1/2} .$$

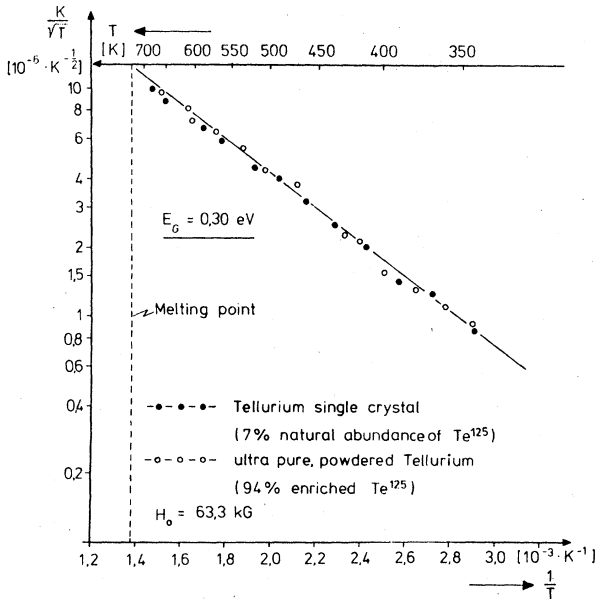

FIG. 2. Knight-shift K times the square root of the inverse temperature of ^{125}Te in tellurium, plotted against the inverse absolute temperature. The straight line fitting the data confirms the validity of the temperature dependence of K as predicted by Eq. (2.21b).

B. Zeeman spin-lattice relaxation measurements

Figure 3 shows a semilogarithmic plot of the Zeeman spin-lattice relaxation rate $1/T_1^Z$ of ^{125}Te as a function of inverse temperature. The measurements were carried out in tellurium single crystals with either a natural abundance of ^{125}Te (7%) or a high concentration of ^{125}Te (94%). To avoid problems associated with the establishment of a single spin temperature, the orientation of the crystals relative to the field $\vec{H}_0$ was chosen in such a way that the three lines of the ^{125}Te spectrum coincide (c axis parallel to $\vec{H}_0$). As demonstrated in Fig. 3, the relaxation rate is independent of the concentration of ^{125}Te. As shown in a previous paper,[6] the relaxation rate is also independent of the strength of the field $\vec{H}_0$.

Contrary to the Knight-shift data presented in Fig. 2, two regions of the T_1^Z vs $1/T$ curve may be distinguished. The temperature variation of the relaxation rate below 420 K is determined by the interaction of the nuclear spins with phonons and conduction electrons. Above 420 K, the slope is markedly higher, indicating that an additional relaxation mechanism is activated. As we shall discuss in detail in a subsequent article, atomic translational diffusion, which modulates the chemical-shift interactions, is responsible for the relaxation process in this region. In our case, in which the three NMR lines coincide, only a diffusion process involving interstitial sites is capable of causing fluctuations in the chemical-shift interactions. Therefore, the energy of 0.58 eV determined from the slope of the high-temperature data in Fig. 3 is found to be associated with the activation energy (formation and migration) of interstitials in tellurium. To obtain the conduction-electron induced part of the relaxation rate from the low-temperature data of Fig. 3, one has to subtract the relaxation rate caused by phonon-spin interactions. As shown by Koma *et al.*,[8] in the case of tellurium, the phonon-induced contribution to the relaxation rate is a Raman two-phonon process. By analogy with the phonon-induced quadrupolar relaxation first calculated by Van Kranendonk,[21] phonons cause the chemical-shift tensor to fluctuate, and this causes fluctuating magnetic fields at the nuclear positions. These fluctuating fields, in turn, give rise to the nuclear magnetic relaxation. Koma *et al.*[8] have shown that this relaxation mechanism is dominant for tellurium in the low-temperature region (20–200 K). From their data, the phonon-induced part of the relaxation rate $(1/T_1)_{ph}$ can be calculated as

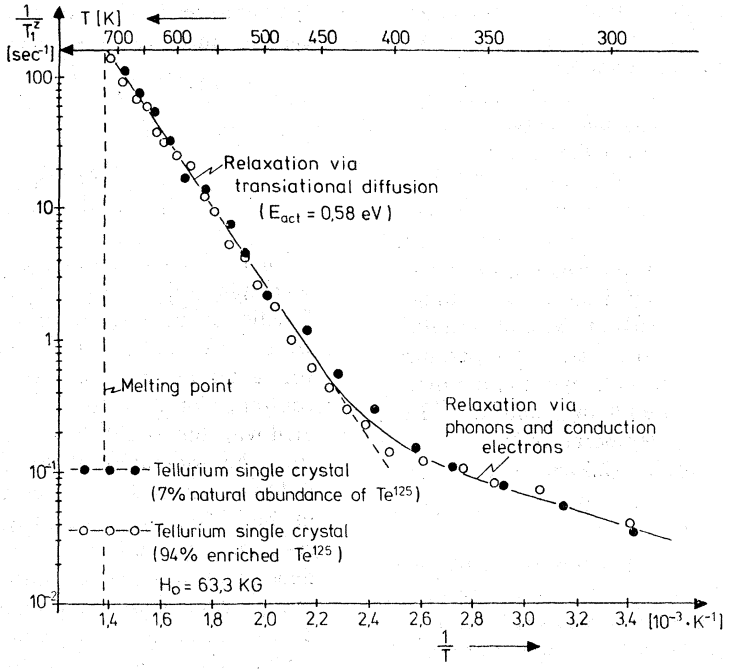

FIG. 3. Zeeman spin-lattice relaxation rate $1/T_1^Z$ of ^{125}Te in tellurium single crystals, as a function of inverse temperature. The c axis of the crystal was aligned parallel to the direction of $\vec{H}_0$, an orientation for which the three lines of the ^{125}Te spectrum coincide.

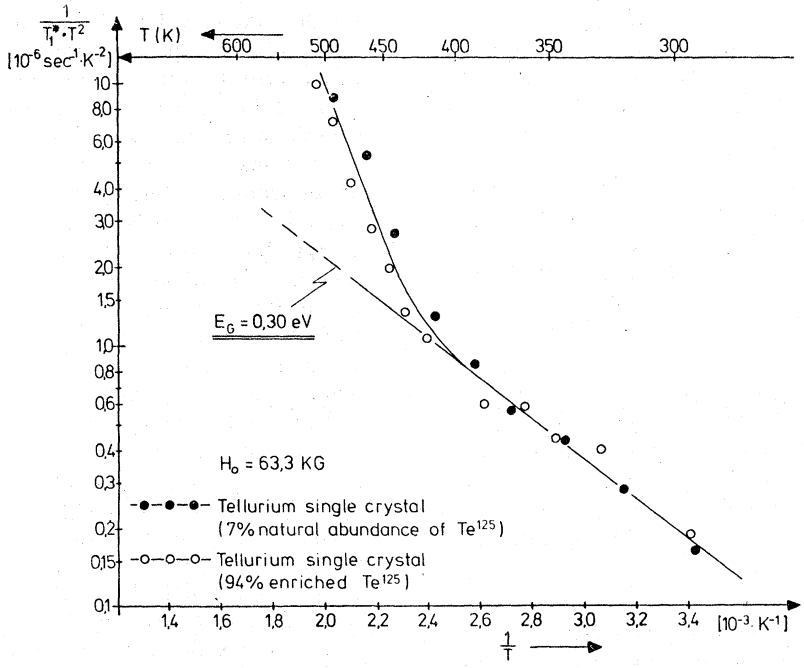

FIG. 4. Arrhenius representation of the phonon-corrected Zeeman relaxation rate $1/T_1{}^*$ times the square of the inverse temperature for ^{125}Te in tellurium, as obtained from Fig. 2. Below 420 K, the data are in agreement with the theoretical relationship (2.21a).

$$(1/T_1)_{ph} = 0.25\times10^{-6}T^2(\text{sec}^{-1}) , \quad (4.2)$$

where T is the temperature in degrees Kelvin.

As shown by Eq. (2.21a), the temperature dependence of the relaxation rate caused by conduction electrons is governed by the relation

$$\frac{1}{(T_1^Z)_e T^2} = A_2 \exp(-E_g/2kT) , \quad (4.3)$$

where A_2 is a temperature-independent constant. Figure 4 shows an Arrhenius representation of the experimental data of Fig. 3 suggested by the above relationship. The relaxation rate $1/T_1{}^*$ in Fig. 4 is defined as $1/T_1{}^* = 1/T_1^Z - (1/T_1)_{ph}$. The slope of the low-temperature (300–420 K) data leads to a gap energy of 0.30 eV, in agreement with the value obtained from our Knight-shift measurements (see Sec. IV A). Furthermore, the data of Fig. 4 yields a value of the coefficient A_2 of

$$A_2 = 69.7\times10^{-6}\,\text{sec}^{-1}\text{K}^{-2} .$$

Combining Eqs. (4.1) and (4.3), the modified Korringa relationship [Eq. (2.22)] can be written as follows:

$$K^2(T_1^Z)_e T = C \exp\left(-\frac{0.30\ \text{eV}}{kT}\right) , \quad (4.4)$$

where the pre-exponential factor $C = A_1^2/A_2$ has been determined experimentally as

$$C_{exp} = 2.7\times10^{-4}\,\text{sec K} .$$

On the other hand, the pre-exponential factor C can be calculated theoretically by means of Eq. (2.22)

$$C = \frac{\hbar}{4k}\left(\frac{\gamma_e}{\gamma_I}\right)^2\left(\frac{m_h{}^*}{m_e{}^*}\right)^{3/4} . \quad (4.5)$$

With $m_h{}^* = 0.5m_0$ and $m_e{}^* = 0.27m_0$ (where m_0 is the mass of the free electron)[1] and taking into account that the average g factor of conduction electrons in tellurium has a value of 9 (instead of 2, as for free electrons[1]), Eq. (4.5) yields

$$C_{theory} = 2.63\times10^{-4}\,\text{sec K} .$$

Obviously, the theoretical value of C agrees quite well with the experimentally determined value. This indicates that the assumption of a Fermi-contact interaction between s-type conduction electrons and nuclear spins (see Sec. II), represents a valid description of the electronic properties of the semiconductor tellurium.

C. Relaxation measurements in the rotating frame

To obtain an experimental value of the coefficient δ in tellurium as introduced by Eq. (2.9), relaxation measurements in the rotating frame were performed on ^{125}Te below 450 K by means of the ADRF technique, as described in Sec. III. The measurements were carried out on a tellurium single crystal with a natural abundance of ^{125}Te. As in all of our T_1 experiments, the c axis of the crystal was parallel to the direction of the magnetic field $\vec{H}_0$. Figure 5 shows $1/T_1$ obtained by ADRF in comparison with the Zeeman relaxation rates obtained in the same single crystal (see Fig. 3). As proposed by Eq. (2.9), the ratio of the two relaxation rates is equal to the coefficient δ. From the low-temperature data presented in Fig. 5, one obtains a value of $\delta \simeq 1.5$, in rough agreement with the theoretical value of 1.8 for a powdered sample as discussed in Sec. II. It should be noted at this point that a value of 1.8 is expected only in cases with direct dipolar interactions between the nuclear spins. In tellurium, the indirect (pseudo-) dipolar interactions cannot be completely neglected, however. The fact that δ is less than two is nevertheless remarkable in that no other δ value this low has been reported for metals in which T_1 is also governed by Fermi-contact interactions. This may support the argument, promoted in Ref. 12, that values of δ in excess of 1.8 are due to quadrupolar effects.

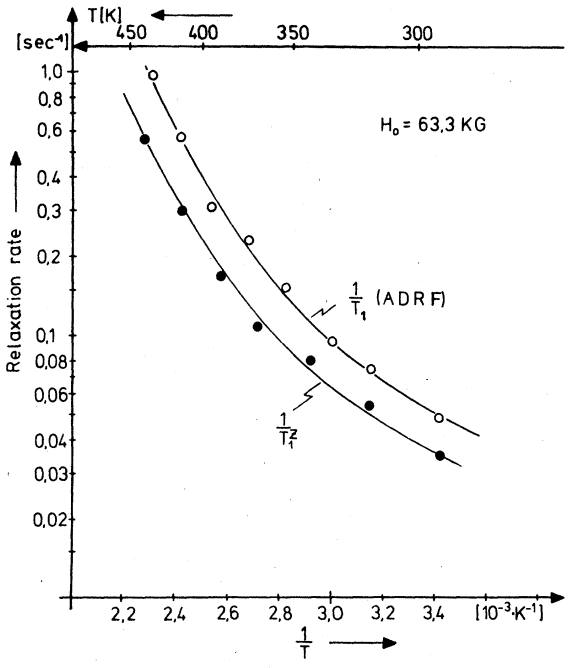

FIG. 5. Comparison between the relaxation rate of ^{125}Te in the rotating frame at zero field (ADRF) $1/T_1$, and the Zeeman relaxation rate $1/T_1^Z$, plotted semilogarithmically vs the inverse temperature. The measurements were carried out on a tellurium single crystal with a natural abundance of ^{125}Te (7%); the c axis was aligned parallel to the direction of $\vec{H}_0$.

ACKNOWLEDGMENTS

We would like to thank Dr. D. Mali for his assistance with the experiments. We gratefully acknowledge financial support from the "Herbert-Quandt-Stiftung". Parts of this work were sponsored by the U.S. DOE.

[1]P. Grosse, *Die Festkorpereigenschaften von Tellur,* Vol. 48 of *Springer Tracts in Modern Physics,* edited by G. Hohler (Springer, New York, 1969).
[2]H. W. Bühren and J. M. Debever, *Physics of Quantum Electronics* (McGraw-Hill, New York, 1966).
[3]W. Hörstel and G. Kretschmar, Phys. Status Solidi 23, 639 (1967).
[4]M. Bensoussan, J. Chem. Phys. 28, 1533 (1967).
[5]A. Koma, Phys. Status Solidi B 56, 655 (1973).
[6]H. Selbach and O. Kanert, Solid State Commun. 20, 609 (1976); and Solid State Commun. 26, 283 (1978).
[7]M. Bensoussan, J. Phys. Chem. Solids 35, 1661 (1964).
[8]A. Koma, A. Hojo, and S. Tanaka, Phys. Lett. A 28, 95 (1968).
[9]A. Abragam, *Principles of Nuclear Magnetism* (Clarendon, Oxford, 1970).
[10]N. Bloembergen, Physica (Utrecht) 20, 1130 (1954).
[11]L. C. Hebel and C. P. Slichter, Phys. Rev. 113, 1504 (1959).
[12]D. Wolf, *Spin Temperature and Nuclear Spin Relaxation in Matter* (Clarendon, Oxford, 1979).
[13]C. P. Slichter, *Principles of Magnetic Resonance* (Harper and Row, New York, 1963).
[14]J. Winter, *Magnetic Resonance in Metals* (Clarendon, Oxford, 1971).
[15]A. G. Anderson and A. G. Redfield, Phys. Rev. 116, 583 (1959).
[16]L. C. Hebel, Solid State Phys. 15, 409 (1963).
[17]T. J. Rowland and F. Y. Fradin, Phys. Rev. 182, 760 (1969).
[18]C. Kittel, *Introduction to Solid State Physics* (Wiley, New York, 1966).
[19]P. Tao-I Chiang, Can. J. Phys. 44, 1195 (1966).
[20]J. U. Arnold and P. Grosse, Phys. Status Solidi B 28, K93 (1968).
[21]F. Van Kranendonk, Physica (Utrecht) 20, 781 (1954).